MARCEL DEKKER, INC. • 270 MADISON AVENUE • NEW YORK, NY 10016



DRUG DEVELOPMENT AND INDUSTRIAL PHARMACY®
Vol. 29, No. 6, pp. 689–700, 2003

# Physical Characterization and Macrophage Cell Uptake of Mannan-Coated Nanoparticles

**Zhengrong Cui, Cheng-Hsuan Hsu, and Russell J. Mumper***

Division of Pharmaceutical Sciences, College of Pharmacy, University of Kentucky, Lexington, Kentucky, USA

## ABSTRACT

Previously, we reported on a cationic nanoparticle-based DNA vaccine delivery system engineered from warm oil-in-water microemulsion precursors. In these present studies, the feasibility of lyophilizing the nanoparticles and their thermal properties were investigated. Also, the binding and uptake of the nanoparticles by a macrophage cell line were studied. The nanoparticles (prior to pDNA coating) were freeze-dried with lactose or sucrose as cryoprotectants. The stability of lyophilized nanoparticles at room temperature was monitored and compared to that of the aqueous nanoparticle suspension. The thermal properties of the nanoparticles were investigated using differential scanning calorimetry (DSC). The nanoparticles, coated or uncoated with mannan as a ligand, were incubated with a mannose receptor positive (MR+) mouse macrophage cell line (J774E), at either 4°C or 37°C to study the binding and uptake of the nanoparticles by the cells. It was found that lactose or sucrose (1–5%, w/v) was required for successful lyophilization of the nanoparticles. After 4 months of storage, the size of lyophilized nanoparticles did not significantly increase while those in aqueous suspension grew by over 900%. Unlike its individual components, emulsifying wax (m.p., ~55°C) and hexadecyltrimethyl ammonium bromide, the nanoparticles showed a melting point of ~90°C. Moreover, the DSC profile of the nanoparticles was different from that of the physical mixture of emulsifying wax and CTAB. After 1 hour incubation at 37°C, the uptake of mannan-coated nanoparticles was 50% higher than that of the uncoated nanoparticles. At 4°C and after one hour, the binding of the mannan-coated nanoparticles by J774E was over 2-fold higher than that of the uncoated nanoparticles. This increase in J774E binding could be abolished by preincubating the cells with free mannan, suggesting that the binding and uptake were receptor-mediated. In conclusion,

*Correspondence: Russell J. Mumper, Ph.D., Assistant Professor of Pharmaceutical Sciences, Assistant Director, Center for Pharmaceutical Science and Technology, College of Pharmacy, University of Kentucky, Lexington, KY 40536-0082, USA; Fax: (859) 323-5985; E-mail: rjmump2@uky.edu.



DOI: 10.1081/DDC-120021318
0363-9045 (Print); 1520-5762 (Online)

www.dekker.com

the nanoparticles were lyophilizable, and lyophilization was shown to enhance the stability of the nanoparticles. DSC provided evidence that the nanoparticles were not a physical mixture of their individual components. Finally, cell binding and uptake studies demonstrated that the nanoparticles have potential application for cell-specific targeting.

*Key Words:* Microemulsion; Stability; Cell binding; Receptor; Lyophilization; Plasmid.

## INTRODUCTION

Nanoparticles have attracted much attention recently primarily due to the fact that these particles have different, and in most of the cases, more desirable chemical, physical, and biological properties. For example, in the pharmaceutical field, nanoparticles have been actively explored as vehicles to deliver both small drug molecules and other macromolecules, such as peptides, proteins, and plasmid DNA.[1] Generally, small drug molecules may reach the desired tissues or cells by diffusion and/or transport mechanisms. In contrast, it is usually difficult to achieve desired amount of macromolecular drugs in certain tissues or cells, such as solid tumors.[2] To effectively treat solid tumors, a defined concentration of drug is usually required in the center of the tumors. However, due to their unique structure, diffusion and/or transport of macromolecular drugs into the center of the tumors are very difficult.[2] Moreover, in the case of plasmid DNA (pDNA)-based vaccine delivery, the pDNA macromolecules are required to be inside the nucleus for the expression of the protein antigens. However, the uptake of pDNA molecules in solution by cells involved in immune responses is usually very poor.[3] Nanoparticles have been proposed as delivery vehicles to better address the aforementioned issues.[4] The immune system has evolved to combat bacteria, viruses, and parasites, which are all particulates. Therefore, it is reasonable that the association of vaccines with microparticles or nanoparticles has resulted in enhanced immune responses.[5–6] In addition, there is also evidence that nanoparticles can induce stronger immune responses than microparticles.[6]

There have been several different methods to prepare nanoparticles comprised of various materials.[7–9] Our laboratories previously reported on a novel method to engineer cationic,[10] neutral,[11] and anionic nanoparticles[12] from warm oil-in-water (O/W) microemulsion precursors. The microemulsions, formed at increased temperature (50–55°C), were comprised of emulsifying wax as the oil phase and different surfactants, either cationic, neutral, or anionic, to engineer nanoparticles with the corresponding surface charge. Nanoparticles were formed by simple cooling of the warm microemulsion precursors at room temperature in the same container. This manufacturing method may have the following advantages, in part: (i) the natural engineering process can easily be adapted to include many different materials, (ii) well-defined and uniform solid nanoparticles may be readily and reproducibly engineered without the use of expensive and/or damaging high-torque mixing, (iii) the engineering process is potentially scalable, (iv) toxic and organic solvents are not required, (v) cell-specific targeting ligand(s) may be readily attached on the surface of these nanoparticles. Hexadecyltrimethyl ammonium bromide (CTAB) was used as a cationic surfactant to engineer cationic nanoparticles (~100 nm), and plasmid DNA was coated on the surface of these preformed nanoparticles to form pDNA-coated nanoparticles.[10] Both an endosomolytic lipid (DOPE) and a potential antigen-presenting cell-targeting ligand (mannan) were successfully incorporated in, or deposited on the surface of, the nanoparticles to modify their in vitro and in vivo performance. Immunization of mice with these pDNA-coated nanoparticles by subcutaneous injection,[10] intradermal injection,[13] intranasal application,[14] and non-invasive topical application on the skin[15] led to enhanced immune responses to an expressed model antigen, β-galactosidase, compared to immunization with "naked" pDNA alone, demonstrating the potential of these nanoparticles as a pDNA-based vaccine delivery system.

However, as previously reported,[10] the size of these cationic nanoparticles prior to pDNA coating was found to increase with time when they were stored as aqueous suspensions, making it necessary to develop a freeze-dried form of the nanoparticles to increase stability. Therefore, one aim of the present studies was to investigate the feasibility of lyophilizing these nanoparticles and to compare the stability of these nanoparticles in lyophilized form with those in aqueous suspension.

The application of cell-specific ligand(s) for targeted delivery is another actively investigated field with the aim to more effectively and/or selectively deliver drugs. Although the mechanisms of induction of immunity after pDNA immunization have not been fully elucidated, recent studies have indicated that direct transfection of antigen-presenting cells (APC) such as dendritic cells (DCs) and macrophages may play an important role.[16] Mouse and human DCs and macrophages have been shown to express a mannose receptor (MR), and this receptor has been exploited to deliver antigens resulting in more robust T-helper type-1 (Th1) and cytotoxic T lymphocyte (CTL) responses.[17–20] For example, Toda et al. (1997) reported that when an HIV-1 DNA vaccine was delivered intranasally using mannan-coated liposomes, the resulting serum IgG and fecal IgA titers were all significantly greater than those resulting after delivery of uncoated liposomes. Moreover, mannan-coated liposomes also led to significantly enhanced CTL responses over uncoated liposomes.[20] As mentioned above, a polysaccharide of mannose (mannan) has been successfully deposited on the surface of these cationic nanoparticles. Nanoparticles were coated with mannan as a ligand to target antigen-presenting cells to enhance the resulting immune responses. As a preliminary step, cell binding and uptake studies were carried out to investigate whether the coating of nanoparticles with mannan can enhance the in vitro binding and/or uptake of the nanoparticles by a mannose receptor positive (MR+) mouse macrophage cell line.[21]

## MATERIALS AND METHODS

### Materials

Emulsifying wax (N.F. grade) was purchased from Spectrum Quality Products, Inc. (New Brunswick, NJ). Hexadecyltrimethyl ammonium bromide (CTAB), lactose, sucrose, and Sephadex G-75 were from Sigma Chemical Co. (St. Louis, MO). Dioleoyl phosphatidyl-ethanolamine (DOPE) and fluorescein-labeled DOPE [1,2-Dioleoyl-sn-Glycero-3-Phosphoethanolamine-*N*-(Carboxyfluorescein)], were purchased from Avanti Polar Lipids, Inc. (Alabaster, AL). {*N*-[2-(Chloesterylcarboxyamino)ethyl]-carbamoylmethyl}mannan (chol-mannan) was purchased from Dojindo Molecular Technologies, Inc. (Gaithersburg, MD).

### Engineering of Cationic Nanoparticles

The cationic nanoparticles were prepared as previously described.[10,15] Briefly, emulsifying wax (2 mg) was melted at 55°C. Seven hundred μL of water was added into the melted wax and stirred until a homogenous milky suspension was obtained. Then, 0.3 mL of CTAB (HLB = 10) solution (50 mM) was added into the homogenate while stirring to obtain a clear microemulsion. Nanoparticles were engineered by simple and direct cooling of this warm microemulsion to room temperature in the same container. DOPE, fluorescein-labeled or unlabeled, was incorporated into the nanoparticles by mixing 100 μg of DOPE (final 5% w/w) with the emulsifying wax (2 mg/mL) prior to microemulsion preparation. Chol-mannan, dissolved in hot water (5 mg/mL), was deposited on the surface of the nanoparticles by mixing 1 mL of the preformed nanoparticle suspension (2 mg/mL) with 250 μg of chol-mannan and stirring at room temperature overnight. Free CTAB and chol-mannan were removed by passing the nanoparticle suspension through a Sephadex G-75 column (14 × 65 mm) using filtered (0.22 μm) water as the mobile phase.[10]

### Physical Characterization of the Cationic Nanoparticles

The nanoparticle size was measured by photon correlation spectroscopy (PCS) using a Coulter N4 Plus Submicron Particle Sizer (Coulter, Miami, FL) by scattering light at 90° at 25°C for 120 s for each 1 mL sample. Particles were diluted with appropriate solution to obtain final counts per sec (cps) ranging from $5 \times 10^4$ to $1 \times 10^6$ as recommended by the manufacturer. The zeta potential of the nanoparticles was measured using a Zeta Sizer 2000 from Malvern Instruments (Southborough, MA).

### Lyophilization of the Cationic Nanoparticles

Before lyophilization, GPC-purified cationic nanoparticles without pDNA were diluted with water or with an aqueous solution of the lactose or sucrose so that the final cryoprotectant concentration varied from 0 to 20% (w/v). The diluted nanoparticle suspensions (1 mL) were then added to glass vials (7 mL) and frozen either at −20°C or −80°C overnight. The various samples were then lyophilized for

24 h on a Labconco Freeze-Dryer (Model 4.5). After lyophilization, vials were sealed and stored at room temperature. Prior to the measurement of particle size, the lyophilized samples were resuspended with deionized and filtered (0.22 μm) water to the original volume.

### Stability of the Cationic Nanoparticles

The cationic nanoparticles, either in aqueous suspension or as lyophilized cake, were stored in sealed glass vials in the dark at room temperature, and their particle sizes were measured after 0, 1, 4, 8, and 16 weeks as described above.

### Differential Scanning Calorimetry (DSC)

DSC analyses were performed using a modulated differential scanning calorimeter TA 2920 DSC from TA Instruments (New Castle, DE). Approximately 4 mg of samples were accurately weighed into the DSC aluminum pans. An empty pan was used as a reference. The samples were cooled to 10°C at a rate of 5°C/min, heated from 10°C to 30°C at a rate of 5°C/min, and equilibrated at 30°C for 10 min. Then, the samples were heated at a rate of 5°C/min from 30°C to 130°C. All experiments were carried out in triplicate to verify reproducibility. The samples were emulsifying wax, physical mixture of the emulsifying wax and CTAB (~1:2.5, w/w), and lyophilized nanoparticles (without cryoprotectant).

### In Vitro Cell Binding and Uptake Studies

A mannose receptor positive (MR+) mouse macrophage cell line (J774E) was obtained from Dr. P. D. Stahl (Washington University, St. Louis, MO) who originally developed the cell line.[21] The cells were grown in Roswell Park Memorial Institute (RPMI) medium (Gibco, BRL) supplemented with 10% fetal bovine serum (FBS, Gibco, BRL) and 100 μg/mL each of penicillin and streptomycin (Sigma). Cell binding and uptake studies were performed with cells that were approximately 80% confluent. Cells were plated in 48-well plates at a cell density of $5 \times 10^5$ cells/well and allowed to grow for 24 h. The cells were then incubated with GPC-purified and fluorescein-labeled nanoparticles, coated or uncoated with mannan, for 0, 5, 10, 30, and 60 min at 4°C or 37°C under 5% $CO_2$. The incubation was terminated by withdrawing the supernatant. The cells were then washed three times with PBS buffer (10 mM, pH 7.4), and lysed by adding 500 μL 1 × Lysis Buffer (Promega, Madison, WI) for 10 min, and then freeze-thawed three times. The cell lysates were diluted with water to 1 mL, and the fluorescence intensity was determined using a F-2000 Fluorescence Spectrophotometer (Hitachi Instruments, Danbury, CT, excitation 497 nm, emission 521 nm). Unlabeled nanoparticles were also incubated at 4°C and 37°C as controls. Incubation at 4°C was undertaken to study the binding of the nanoparticles on the macrophage cell surface. Cell binding and uptake of the nanoparticles were reported as the ratio of the fluorescence determined in the cell lysates to the total amount of fluorescence added. A standard curve of fluorescence intensity vs. the amount of fluorescein-labeled nanoparticles was constructed.

### Statistical Analyses

Except where mentioned, all statistical analyses were completed using a one-way analysis of variances (ANOVA) followed by pair-wise comparisons with Fisher's protected least significant difference procedure (PLSD). A p-value of $\leq 0.05$ was considered to be statistically significant.

## RESULTS AND DISCUSSION

Previously, we reported on a novel method to engineer cationic nanoparticles from warm O/W microemulsion precursors for potential DNA vaccine delivery and targeting.[10] The microemulsions, formed at increased temperature (50–55°C), were comprised of emulsifying wax (2 mg/mL) as the oil phase and a cationic surfactant (CTAB, 15 mM). Nanoparticles were formed by simple cooling of the warm microemulsion precursors at room temperature. Plasmid DNA was then coated on the surface of these nanoparticles to form pDNA-coated nanoparticles. Both an endosomolytic lipid (DOPE) and a potential antigen-presenting cell-targeting ligand (mannan) were successfully incorporated in, or deposited on the surface of, the nanoparticles to modify their in vitro and in vivo performance. Immunization of mice with these pDNA-coated nanoparticles by subcutaneous, intradermal, intranasal, and noninvasive topical routes resulted in enhanced immune responses to an expressed model antigen, β-galactosidase, compared to immunization

with "naked" pDNA alone, demonstrating the potential of these nanoparticles as a pDNA vaccine delivery system.[10,13–15] However, as previously reported,[10] although the composition of the nanoparticles was optimized to obtain the smallest and most stable nanoparticles, the size of these optimized cationic nanoparticles prior to pDNA coating still increased with time when stored as suspensions. Thus, it was necessary to develop methods, such as lyophilization, for long term storage.

## Lyophilization of the Cationic Nanoparticles

Numerous studies have shown the protective effect of disaccharides in preventing particle aggregation during the freeze-drying process.[22–24] Therefore, before lyophilization, a simple freeze-thaw experiment was carried out to determine whether cryoprotectant was required for the lyophilization of these cationic nanoparticles, and if so, to select the appropriate cryoprotectant and concentration for further lyophilization studies. Table 1 shows the results from the freeze-thaw experiments. Two disaccharides, lactose and sucrose with concentrations ranging from 0 to 20% (w/v), were used to investigate the stability of these GPC-purified nanoparticles (prior to pDNA coating) after freeze-thawing procedure under fast (−80°C) and slow (−20°C) freezing conditions. The diameter of the purified nanoparticles before freeze-thawing was $98 \pm 5$ nm (mean ± S.D., $n = 3$). It is apparent from Table 1 that a cryoprotectant was required to prevent aggregation of the nanoparticles in the freeze-thawing step. In fact, as low as 1% (w/v) of either lactose or sucrose in the suspension was enough to prevent the nanoparticles from subsequent aggregation upon thawing. Lactose and sucrose at the same concentration were equally effective in preventing aggregation. Moreover, Table 1 also demonstrated that without any cryoprotectant fast freezing resulted in less aggregation of the thawed nanoparticles than slow freezing. However, with cryoprotectant, the rate of freezing did not affect the resulting particle size of the thawed nanoparticles.

Nanoparticles subjected to freezing at −80°C were then lyophilized for 24 h, and the lyophilized cakes were reconstituted with an equal volume of water. One minute of manual shaking was sufficient to ensure complete reconstitution of the lyophilized nanoparticles. Fig. 1 shows the sizes of the reconstituted nanoparticles. As expected, without any cryoprotectant, the diameter of the reconstituted nanoparticles was 300–450% greater than their original size. The addition of cryoprotectants improved the situation, and less aggregation resulted. The inclusion of either lactose or sucrose at concentrations of 1, 2, or 5% (w/v) was equally effective in maintaining the particle size. However, a further increase in the concentration of the cryoprotectants had the tendency to lead to increased particle size after reconstitution. For example, the size of the reconstituted nanoparticles increased ~1.8-fold over that of their original size (i.e., from 100 to ~180 nm) when 20% (w/v) lactose was used.

***Table 1.*** Effect of cryoprotectant and freezing temperature on the resulting particle size of the thawed nanoparticles.

| | Disaccharides (freezing temperature) | | | |
|---|---|---|---|---|
| % (w/v) | Lactose (−20°C) | Lactose (−80°C) | Sucrose (−20°C) | Sucrose (−80°C) |
| 0 | 1850 ± 305 (1.518)[a] | 384 ± 162 (0.609)[a,b] | 1954 ± 922 (2.025)[a] | 386 ± 160 (0.541)[a,b] |
| 1 | 77 ± 26 (0.212) | 118 ± 47 (0.418) | 94 ± 32 (0.207) | 98 ± 34 (0.225) |
| 2.5 | 88 ± 30 (0.221) | 101 ± 34 (0.201) | 99 ± 35 (0.248) | 97 ± 33 (0.209) |
| 5 | 96 ± 33 (0.206) | 103 ± 39 (0.329) | 104 ± 32 (0.146) | 103 ± 36 (0.231) |
| 10 | 116 ± 39 (0.223) | 120 ± 42 (0.237) | 118 ± 40 (0.207) | 116 ± 40 (0.221) |
| 20 | 147 ± 52 (0.249) | 150 ± 54 (0.265) | 149 ± 54 (0.276) | 144 ± 36 (0.084) |

GPC-purified cationic nanoparticle suspensions with no pDNA were frozen at −20°C or −80°C overnight with different concentrations of cryoprotectants, lactose or sucrose, and then thawed at room temperature. The original particle size of the cationic nanoparticles was 98 ± 5 nm. Data reported are the mean ± standard deviation (polydispersity index) of the reconstituted nanoparticles. (a) indicates that within the same column, the result from a sample without the cryoprotectant was significantly different from those with the cryoprotectant. (b) indicates that freezing at −80°C and −20°C without cryoprotectant resulted in significantly different particle sizes.

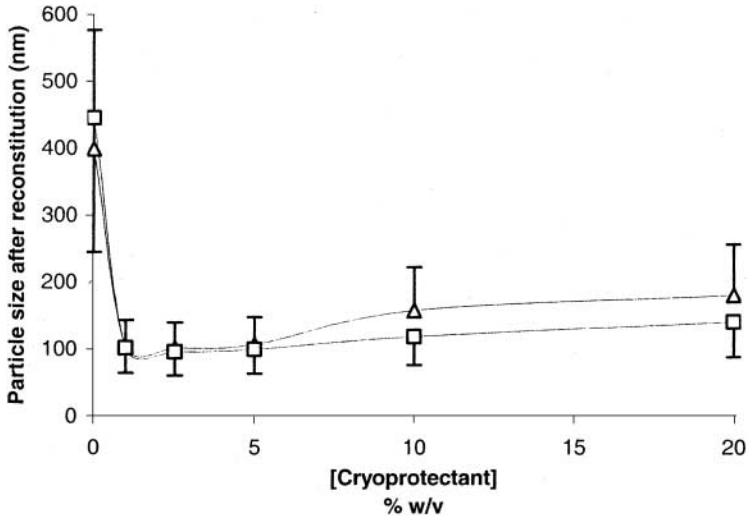


*Figure 1.* The particle size of the reconstituted nanoparticles after lyophilization with different concentrations of cryoprotectant, sucrose (□) or lactose (△). Data reported are the mean ± standard deviation. The nanoparticles were engineered from microemulsion precursors comprised of CTAB (15 mM) and emulsifying wax (2 mg/mL). The nanoparticles were GPC-purified prior to lyophilization.

The protective effect of the disaccharides may be attributed to the ability of the sugars to form a glassy amorphous "shell" around the particles, preventing the particles from adhering together during the removal of water.[25–26] In general, one of the critical analyses of lyophilized products includes the visual observation of the final volume and appearance of the lyophilized cake. One of the desired characteristics of a freeze-dried pharmaceutical form includes an intact cake occupying the same volume and size as the original frozen mass.[27] In the present study, the cakes that contained a lower concentration of the disaccharides (1–5%, w/v) provided a fluffy, stable cake. However, the cakes that contained 20% (w/v) of the disaccharides, especially sucrose, appeared to be hard, dense, and slightly difficult to reconstitute. Since the cationic nanoparticles were suspended in 10% (w/v) lactose solution in previous in vivo mouse studies,[12–15] and the lyophilization experiments in Table 1 and Fig. 1 showed that $< 5\%$ (w/v) of lactose provided improved reconstitution ability, 5% (w/v) of lactose was then selected for further studies.

Previous studies showed that there was a strong correlation between the percent increase of the cationic nanoparticle size in aqueous suspension (an indication of the stability of the nanoparticles) over time and the final CTAB concentration used to prepare the nanoparticles.[10] The correlation was a second-order polynomial with a $R^2 = 0.995$. In fact, the nanoparticles having the highest stability in aqueous suspension were those prepared with a final CTAB concentration of around 15 mM, which were then used for subsequent studies.[10] However, even with this optimized CTAB concentration, the nanoparticles still grew in aqueous suspension, strongly indicating the need for an alternative method to store the nanoparticles. Fig. 2 shows the results of a long-term stability study for the nanoparticles. As expected, when stored as aqueous suspensions in 5% (w/v) lactose, the diameter of the nanoparticles increased by over 900% in 4 months at room temperature. In contrast, when stored as lyophilized cakes, no significant growth was observed in the same period at room temperature, strongly demonstrating that lyophilization is a suitable method to maintain the stability of these cationic nanoparticles. For future studies, the nanoparticles may then be prepared, purified, lyophilized and stored. The lyophilized cake can then be reconstituted with an appropriate vehicle prior to use.

## Differential Scanning Calorimetry (DSC)

Previous studies of the nanoparticles using photon correlation spectroscopy, electrophoretic light scattering, and transmission electron microscopy have demonstrated the spherical nature of the cationic nanoparticles.[10] However, a study on the interactions between the composition molecules of

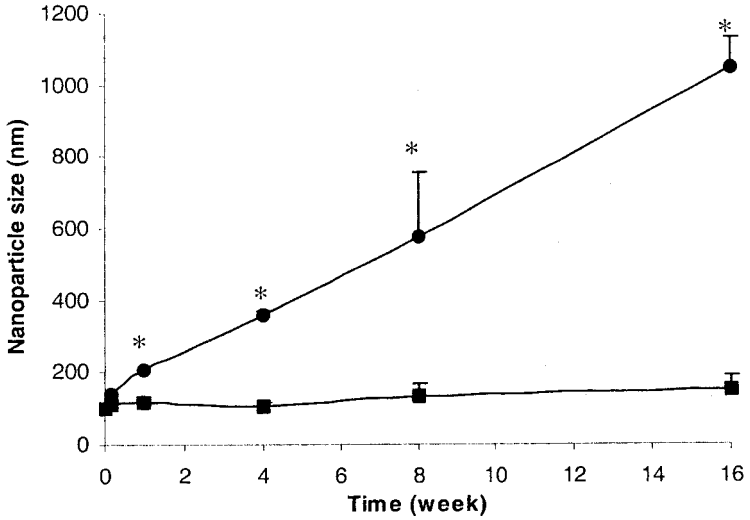


***Figure 2.*** Stability of the GPC-purified cationic nanoparticles (prior to pDNA coating) stored in dark at room temperature either in 5% (w/v) lactose suspension (●) or as lyophilized cake (■). Data reported are the mean ± standard deviation ($n = 3$). * indicates that the size of the nanoparticles stored in aqueous suspension was different from that stored as lyophilized cake after the same period of storage.

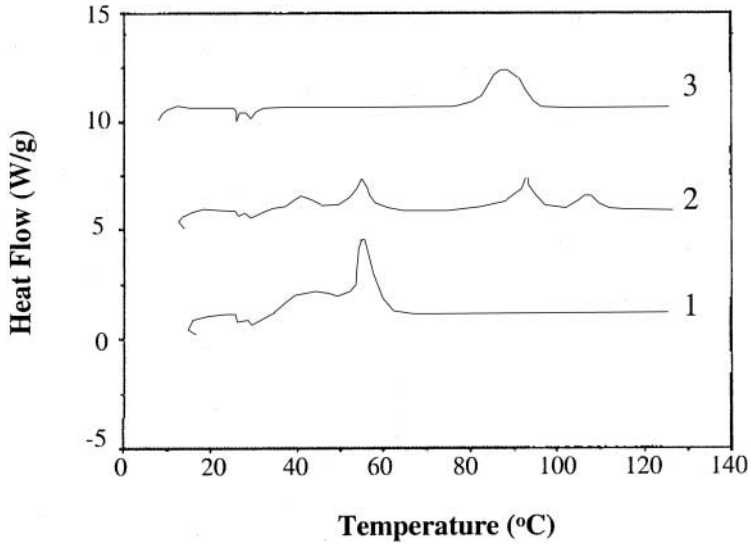


***Figure 3.*** DSC profiles of emulsifying wax (**1**), physical mixture of the CTAB and emulsifying wax (**2**), and the lyophilized nanoparticles (**3**). The nanoparticles were engineered from microemulsion precursors comprised of CTAB (15 mM) and emulsifying wax (2 mg/mL). For **2** and **3**, the ratios (w/w) of the emulsifying wax and CTAB were the same. The melting point of CTAB was reported to be 230°C.

the nanoparticles may also provide useful information about the nanoparticles. DSC is a thermal analytical technique that measures the temperature and heat flow associated with transitions in materials as a function of time. DSC results provide useful information about the physical and chemical changes that involve endothermic or exothermic process or changes in heat capacity.[28] In the present studies, DSC experiments were useful to understand potential emulsifying wax and CTAB interactions in the nanoparticles and the behavior of the mixture. As shown in Fig. 3, the DSC profiles of emulsifying wax alone showed an apparent endothermic peak at about 55°C, corresponding to its known melting point.

The melting point of CTAB was reported to be 230°C. The profile of the physical mixture of emulsifying wax and CTAB showed three small endothermic peaks. In contrast, the profile of the lyophilized powder of the cationic nanoparticles showed a single peak around 90°C, suggesting the existence of unique molecular interactions in these nanoparticles. Taken together, these DSC profiles demonstrated that the cationic nanoparticles, which were engineered from warm microemulsion precursors comprised of emulsifying wax and CTAB, were not a physical mixture of their individual components.

## Cell Binding and Uptake

Targeted delivery of drugs and vaccines through cell-specific ligands has been actively investigated for many years. To effectively elicit immune responses, the thymus-dependent (TD) antigens must be presented by the professional antigen-presenting cells to the T cells. There are three kinds of professional antigen-presenting cells, including dendritic cells (DC), macrophages, and B lymphocytes. DCs and macrophages express high levels of mannose receptor (MR) and mannose receptor-related receptor (MRRR) that are used by the cells for endocytosis and phagocytosis of a variety of antigens that expose mannose residues.[17] Following ligand binding, internalization, and release of the cargo, the mannose receptor is recycled and transported back to the cell surface. Mannose, as a ligand for the mannose receptor on the surface of the antigen-presenting cells, has been successfully explored to deliver antigens resulting in more robust Th1 and CTL responses.[17–20] For example, Apostolopoulos et al. (2000) reported ex vivo targeting of the macrophage mannose receptor generated anti-tumor (adenocarcinomas) CTL responses.[19] The authors showed that murine mannose receptor bearing macrophages derived from peritoneal exudate cells and cultured ex vivo with a mannan-linked protein-based adenocarcinomas antigen, after adoptive transfer, efficiently presented the antigen to T cells, leading to the generation of high frequency of CTL and protection from tumor challenge. Moreover, it was found that targeting the mannose receptor was crucial to obtain high frequency CTL since without the mannan linkage, the frequency of CTL to the antigen was very low.[19]

It was our intent to use mannan as a ligand on the surface of these novel nanoparticles to target DNA vaccines to antigen-presenting cells, and therefore, to potentially enhance the resulting immune responses. As a preliminary step, cell binding and uptake studies were carried out to investigate whether the coating of nanoparticles with mannan can enhance the in vitro binding and/or uptake of the nanoparticles by a MR+ mouse macrophage cell line.[21] J774E is a macrophage cell line derived by Diments, Leech, and Stahl from J774.[21] J774E was shown to over express mannose receptor, and has been used to study the binding or uptake of bacteria or viruses to macrophages.[29–30] Shown in Fig. 4A are the binding and/or uptake of the mannan-coated or uncoated nanoparticles by macrophages after different periods of incubation. At 4°C, receptor mediated endocytotic and phagocytotic processes are no longer active. Therefore, any association of the nanoparticles with the macrophages should be due to surface binding, both receptor specific and nonspecific. Within only ~5 min, the binding of the uncoated nanoparticles to the J774E cells reached saturation. In contrast, binding of the mannan-coated nanoparticles to the J774E cells reached saturation after 20 min of incubation. Finally, after 60 min of incubation, the binding of the mannan-coated nanoparticles by the macrophages was ~90% higher than that of the uncoated nanoparticles (Fig. 4B). Of importance, since the nanoparticles were positively charged, nonspecific binding between the nanoparticles and the cells was relatively high. In the present case, $2.2 \pm 0.1\%$ of nonspecific binding between the uncoated nanoparticles and the macrophage cells was observed. Coating of the polysaccharide (mannan) on the surface of the nanoparticles may increase the binding of the nanoparticles to the macrophages, but may also "shield" some of the positive charges on the surface of the nanoparticles and therefore decrease the binding. In fact, the particle size and zeta potential of the mannan-coated nanoparticles in the present studies were $126 \pm 30$ nm and $27.6 \pm 4$ mV, respectively, while that of the uncoated nanoparticles were $98 \pm 5$ nm and $59.5 \pm 5.0$ mV, respectively. Therefore, the $4.2 \pm 0.2\%$ of binding observed in the present studies probably underestimated the receptor-specific binding between the mannan-coated nanoparticles and the MR+ macrophage cells.

As expected, when the nanoparticles were incubated with the cells at 37°C, enhanced cell association of the nanoparticles was observed (Fig. 4A). For example, after 60 min of incubation, an additional 45% and 68% of the mannan-coated nanoparticles and uncoated nanoparticles were found to be asso-

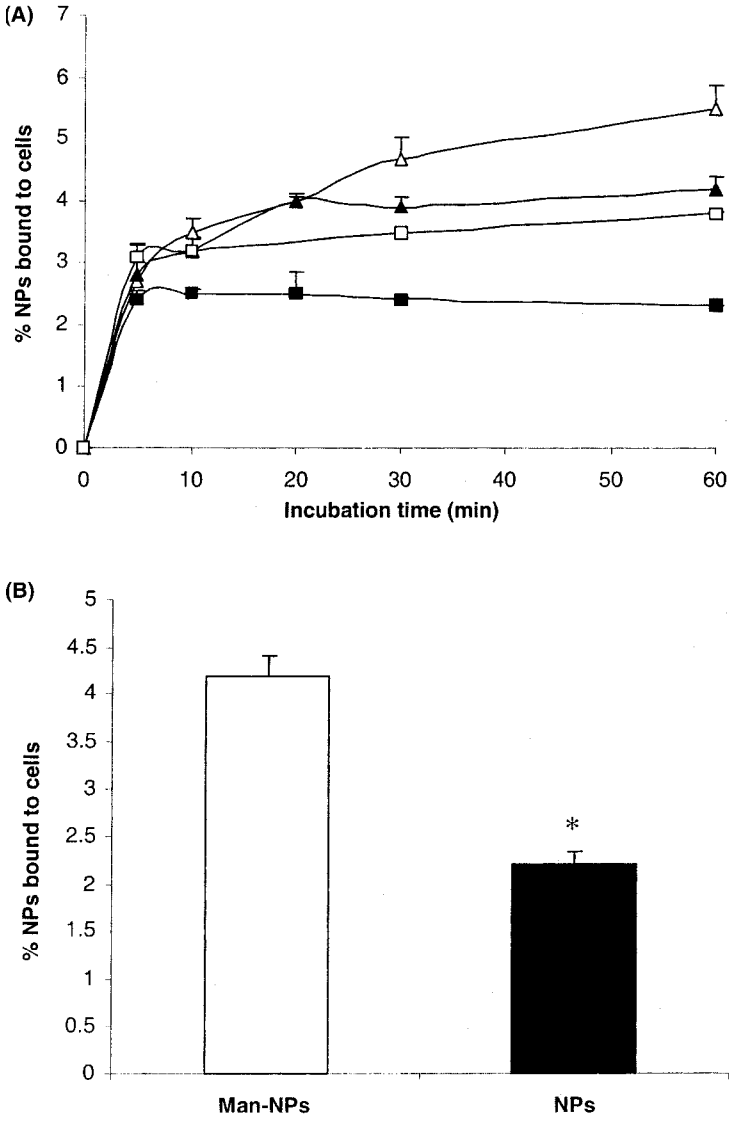


***Figure 4.*** (A) The binding and uptake of the mannan-coated or uncoated nanoparticles by mouse macrophage J774E cells after incubating for various times. The samples used were mannan-coated nanoparticles incubated at 4°C (▲) or at 37°C (△), or uncoated nanoparticles at 4°C (■) or 37°C (□). (B) The binding of nanoparticles to J744E cells. Mannan-coated nanoparticles (Man-NPs) or uncoated nanoparticles (NPs) were incubated for 60 min with J774E cells at 4°C. * indicates that the result of Man-NPs was significantly different from that of NPs. Data reported are the mean ± S.D. ($n = 3$).

ciated with the macrophage cells, respectively. These enhancements likely resulted from the internalization of the particles. Moreover, there was a net 48% increase in the total cell-associated mannan-coated nanoparticles over the uncoated nanoparticles. The relative low (4–5%) binding and/or uptake of the nanoparticles even after saturation observed in the present studies was most likely due to the high concentration of fluorescein-labeled nanoparticles used in these studies. Analyses revealed that a 4% binding of the nanoparticles by the J774E cells meant that there were approximately 40,000–50,000 nanoparticles (~100 nm in diameter) associated with one J774E cell. It was calculated that one single nanoparticle had approximately 10 mannan ligands coated on its surface. For comparison, the estimated number of mannose-dependent receptors for glucocerebrodidase on murine and human macrophages is 500,000 per cell, and that of the number of binding sites for the classical ligand of the mannose receptor (mannose-bovine serum albumin) is approximately 20,000 per macrophage cell.[31]

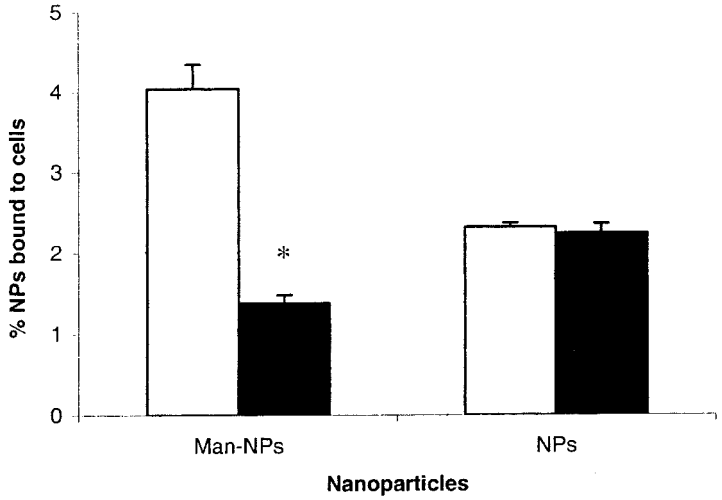


***Figure 5.*** The binding of mannan-coated or uncoated nanoparticles to J774E cells after 60 min of incubation at 4°C. Before the addition of the nanoparticles, the cells were incubated with 0 (white bars) or 50 μg (black bars) of free chol-mannan at 4°C for 30 min. Data reported are the mean ± S.D. ($n = 3$). * indicates that the result of the binding of Man-NPs with 50 μg of free chol-mannan was significantly different from that without free chol-mannan. For uncoated nanoparticles, preincubation with free chol-mannan did not significantly affect the binding of the nanoparticles by the macrophages.

To further confirm whether the binding of the mannan-coated nanoparticles with the macrophage cells was receptor-mediated, the macrophages were preincubated with increasing amounts of free chol-mannan (0 and 50 μg) for 30 min at 4°C prior to the addition of the mannan-coated or uncoated nanoparticles. As shown in Fig. 5, the free chol-mannan successfully prevented the binding of the mannan-coated nanoparticles by the cells. In fact, when 50 μg of free chol-mannan was added before the addition of the mannan-coated nanoparticles, the binding was decreased from ~4% to $1.38 \pm 0.10\%$. This lower binding percent may be the actual nonspecific binding value for the mannan-coated nanoparticles to the macrophages since, by definition, nonspecific binding is the extent of binding of the mannan-coated nanoparticles in the presence of excess amount of free mannan.[32] As expected, in the case of uncoated nanoparticles, pre-incubation with free chol-mannan did not inhibit the binding of the uncoated nanoparticles by the macrophages (Fig. 5).

## CONCLUSIONS

It was found in the present studies that previously reported cationic nanoparticles were lyophilizable, and lyophilization was shown to enhance the stability of the nanoparticles. DSC provided evidence that the nanoparticles were not a physical mixture of their individual components. Finally, cell binding and uptake studies demonstrated that the nanoparticles have potential application for cell-specific targeting.

## REFERENCES

1. Douglas, S.J.; Davis, S.S.; Illum, L. Nanoparticles in drug delivery. Crit. Rev. Ther. Drug Carrier Syst. **1987**, *3*, 233–261.
2. Dubernet, C.; Fattal, E.; Couvreur, P. Nanoparticulate controlled release systems for cancer therapy. In *Handbook of Pharmaceutical Controlled Release Technology*; Wise, D.L., Ed.; Marcel Dekker, Inc.; New York, 2000; 271–285.
3. Mumper, R.J.; Ledebur H.C., Jr. Dendritic cell delivery of plasmid DNA: application for controlled nucleic acid-based vaccines. Mol. Biotech. **2001**, *19*, 79–95.
4. Kreuter, J. Nanoparticles and microparticles for drug and vaccine delivery. J. Anat. **1996**, *189*, (Pt 3):503–505.
5. O'Hagan, D. Recent advances in vaccine adjuvants for systemic and mucosal administration. J. Pharm. Pharmacol. **1997**, *49*, 1–10.

6. Singh, M.; Briones, M.; Ott, G.; O'Hagan, D. Cationic microparticles: a potent delivery system for DNA vaccines. Proc. Natl. Acad. Sci. USA **2000**, *97*, 811–816.
7. Muller, R.H.; Jacobs, C.; Kayser, O. Nanosuspensions as particulate drug formulations in therapy rationale for development and what we can expect for the future. Adv. Drug Del. Rev. **2001**, *47*, 3–19.
8. Ravi Kumar, M.N.V. Nano and microparticles as controlled drug delivery devices. J. Pharm. Pharmaceut. Sci. **2000**, *3*, 234–258.
9. Muller, R.H.; Mader, K.; Gohla, S. Solid lipid nanoparticles (SLN) for controlled drug delivery—a review of the state of the art. Eur. J. Pharm. Biopharm. **2000**, *50*, 161–177.
10. Cui, Z.; Mumper, R.J. Genetic immunization using nanoparticles engineered from microemulsion precursors. Pharm. Res. **2002**, *19*, 939–946.
11. Oyewumi, M.O.; Mumper, R.J. Gadolinium-loaded nanoparticles engineered from microemulsion templates. Drug Dev. Ind. Pharm. **2002**, *28*, 317–328.
12. Cui, Z.; Mumper, R.J. Coating of cationized protein on engineered nanoparticles results in enhanced immune responses. Int. J. Pharm. **2002**, *238*, 229–239.
13. Cui, Z.; Mumper, R.J. Intradermal immunization with novel pDNA-coated nanoparticles via a needle-free injection device. AAPS Annual Meeting and Exposition, Toronto, Ontario, Canada, November 10–14, 2002.
14. Cui, Z.; Mumper, R.J. Intranasal administration of plasmid DNA-coated nanoparticles results in enhanced immune responses. J. Pharm. Pharmacol. **2002**, *54*, 1159–1203.
15. Cui, Z.; Mumper, R.J. Topical immunization using nanoengineered genetic vaccines. J. Control. Rel. **2002**, *81*, 173–184.
16. Donnelly, J.J.; Friedman, A.; Martinez, D.; Montgomery, D.L.; Shiver, J.W.; Motzel, S.; Ulmer, J.B.; Liu, M. Regulatory role for macrophage migration inhibitory factor in acute respiratory distress syndrome, Nat. Med. **1998**, *1*, 583–587.
17. Jordens, R.; Thompson, A.; Amons, R.; Koning, F. Human dendritic cells shed a functional, soluble form of the mannose receptor. Int. Immunol. **1999**, *11*, 1775–1780.
18. Engering, A.J.; Cella, A.M.; Fluitsman, D.; Brockhaus, M.; Hoefsmit, E.M.; Lanzavecchia, A.; Pieters, J. The mannose receptor functions as a high capacity and broad specificity antigen receptor in human dendritic cells. Eur. J. Immunol. **1997**, *27*, 2417–2425.
19. Apostolopoulos, V.; Barnes, N.; Pietersz, G.A.; McKenzie, I.F.C. Ex vivo targeting of the macrophage mannose receptor generates anti-tumor CTL responses. Vaccine **2000**, *18*, 3174–3184.
20. Toda, S.; Ishii, N.; Okuda, E.; Kusakabe, K.I.; Arai, H.; Hamajima, K.; Gorai, I.; Nishioka, K.; Okuda, K. HIV-1-specific cell-mediated immune responses induced by DNA vaccination were enhanced by mannan-coated liposomes and inhibited by anti-interferon-$\gamma$ antibody. Immunology. **1997**, *92*, 111–117.
21. Diments, S.; Leech, M.S.; Stahl, P.D. Generation of macrophage variants with 5-azacytidine: selection for mannose receptor expression. J. Leuk. Biol. **1987**, *42*, 485–490.
22. Doebbler, G.F. Cryoprotective compounds. Cryobiology. **1966**, *3*, 2–11.
23. Crowe, L.M.; Womersley, C.; Crowe, J.H.; Reid, D.; Appel, L.; Rudolph, A.S. Prevention of fusion and leakage in freeze-dried liposomes by carbohydrates. Biochem. Biophys. Acta. **1986**, *236*, 289–296.
24. Crowe, L.M.; Crowe, J.H. Stabilization of dry liposomes by carbohydrates. Dev. Biol. Stand. **1991**, *74*, 285–294.
25. Carpenter, J.F.; Pikal, M.J.; Chang, B.S.; Randolph, T.W. Rational design of stable lyophilized protein formulations: some practical advice. Pharm. Res. **1997**, *14*, 969–974.
26. Ford, A.W.; Dawson, P.J. The effect of carbohydrate additives in the freeze-drying of alkaline phosphatase. J. Pharm. Pharmacol. **1993**, *45*, 86–93.
27. Snowman, J.W. Freeze drying of sterile products. In *Sterile Pharmaceutical Manufacturing: Applications for the 1990's*; Groves, M.J., Olson, W.P., Anisfeld, M.H., Eds.; Interpharm Press: Buffalo Grove, 1991; 79–108.
28. Ford, J.L.; Timmins, P. *Pharmaceutical Thermal Analysis*; Ellis Horwood: Chichester, 1989.
29. Kuo, C.; Puolakkainen, M.; Lin, T.; Witte, M.; Campbell, L. A. Mannose-receptor positive and negative mouse macrophages differ in their susceptibility to infection by *Chlamydia* species. Microb. Pathogen. **2002**, *32*, 4033–4048.
30. Reading, P.C.; Miller, J.L.; Anders, E.M. Involvement of the mannose receptor in

infection of macrophages by influenza virus. J. Viol. **2000**, *74*, 5190–5197.

31. Sato, Y.; Beutler, E. Binding, internalization, and degradation of mannose-terminated glucocerebrosidase by macrophages. J. Clin. Invest. **1993**, *91*, 1909–1917.
32. Robbins, J.C.; Lam, M.H.; Tripp, C.S.; Bugianesi, R.L.; Ponpipom, M.M.; Shen, T.Y. Synthetic glycopeptide substrates for receptor-mediated endocytosis by macrophages. Proc. Natl. Acad. Sci. USA **1981**, *78*, 7294–7298.